In: Progress in Mathematical Biology Research
Editor: James T. Kelly, pp. 1-27
ISBN 978-1-60456-171-5
© 2007 Nova Science Publishers, Inc.

*Chapter 1*

# MATHEMATICAL MODELLING OF HANTAVIRUS: FROM THE MEAN FIELD TO THE INDIVIDUAL LEVEL

***Guillermo Abramson****
Statistical and Interdisciplinary Physics Group
CONICET and Instituto Balseiro
Centro Atómico Bariloche, 8400 Bariloche, Argentina

**Abstract**

I review recent mathematical models of the epizootic of Hantavirus in mice populations. The models are mainly based on field observations of *Peromyscus maniculatus* populations in New Mexico, which hosts Sin Nombre virus. The sporadic disappearance of the infection during times of adverse conditions is explained as a phase transition controlled by the environment. Refinements of the model allow to include the effect of non-host competitors, as well as to assess the validity of the diffusion transport. A stochastic model, based on individual interactions, is also analyzed. We compare its macroscopic limit with the mean field model, and discuss some phenomena inherent to stochastic systems: the role of fluctuations, extinctions and stabilization of oscillations.

## 1 Introduction

In 1993 an outbreak of a severe and unknown disease occurred in the North American Southwest, striking with a mortality in excess of 50%. Shortly afterwards, Sin Nombre virus (Bunyaviridae: Hantavirus), the first Hantavirus to be discovered in the New World, was identified as the infectious agent, and the very common deer mouse (*Peromyscus maniculatus*) as its host and reservoir [1]. Since then, numerous new Hantaviruses have been discovered throughout the Americas, each one hosted by a single mouse species, and many of them responsible for severe human pathology. An interdisciplinary effort has been devoted to understand the zoonosis, with the ultimate goal of correctly assessing the human risk.

*E-mail address: abramson@cab.cnea.gov.ar. Web: http://cabfst28.cnea.gov.ar/∼abramson.

As a result of this effort, a large amount of knowledge has been collected about the Hantaviruses of the Americas, while also a great deal is still ignored or just conjectured. It is known that each species of Hantavirus is almost exclusively associated with a single rodent reservoir, and that human disease caused by these pathogens—Hantavirus Pulmonary Syndrome, HPS—can range from mild to very severe. The infection does not produce any clinical manifestation in the mice, which are asymptomatic carriers. Wild populations of host mice usually harbor a varying proportion of infected animals. They are mostly adult males, and typically the most battered ones, from which it has been conjectured that contagion takes place by direct contact during fights. Infected females transmit their antibodies to newborns, who are thus protected from infection until they are weaned and become susceptible. Infected mice, it also seems, remain infected and infectious for their whole life (wild mice have short lives, with the luckier ones living a couple of years).

It has been observed that the outbreaks of HPS in the North American Southwest in 1993 and again in 1998-2000 were associated with the El Niño-Southern Oscillation (ENSO) phenomenon. El Niño—the warm phase of the ENSO—is accompanied by increased fall-spring precipitation in the arid and semi-arid regions of New Mexico and Arizona, in turn initiating a greater production of food resources for rodents: seeds, berries, nuts, insects. A "trophic cascade" is triggered, which leads to greater reproduction in rodents and, within a year, to large increases in rodent densities. At these higher densities, rodents disperse across the landscape ("ratadas," as they are called in Latin American countries), and come into contact with humans in homes and businesses. An increase in the density of infected rodents was observed one year after the peak rodent densities, suggesting that a "wave" of virus infection was following the "wave" of rodent dispersal.

During times of adverse environmental conditions, a complete disappearance of the disease from local populations has been observed, as well as its eventual reappearance when conditions change.

In recent years, a simple mathematical model of this epizootic has been proposed and analyzed by me and others [2, 3, 4, 5, 6, 7], with the purpose of providing a theoretical framework for the ecological and epidemiological findings. A complete mathematical description of the dynamics of the biological system, comprising the virus, the mice, the humans and the environment, would be a daunting task. Instead, our study attempted to extract a few major ingredients, based on observed features of the mice population. Our analysis proceeded from two conspicuous characteristics of the disease, both originating in the fact that environmental conditions strongly affect the dynamics and persistence of the infection. The first one is that the infection can, occasionally, completely disappear from a local population if environmental conditions get inadequate, only reappearing sporadically or when conditions change [9, 10, 11]. The driving environmental factors can be droughts, El Niño episodes, human activity, etc. The second one is a spatial characteristic: the focality that seems to maintain the infection in "reservoir" populations [9]. Contracting and expanding as the environment change [12], these populations can carry the infection to other places in the form of epidemic waves. The model is able to explain these field observations as environmentally controlled phase transitions. It provides an analytical support to the biological hypothesis of a trophic cascade [12].

In this Chapter I review this model, as well as refinements and extensions that are of more general application. First, an account of the mean field model will be given, including

several peculiarities of the Hantavirus-rodent association, and the role of the spatiotemporal patterns of the environment on the prevalence of the infection. Refinements of the model allow to include the effect of non-host competitors [6], as well as to assess the validity of the diffusion transport [13, 14, 15]. The existence of a competing species has an important effect on the reduction of the prevalence of the infectious agent in the host population. The competitive pressure of the second species leads to reduction or complete elimination of the infection. The transition between the disappearance of the infection and its presence occurs at a critical value of the competitors population, also resembling a second order phase transition in a statistical system.

The spatially extended mean field model is reviewed next. It has been set up, as customary, as a reaction-diffusion system. The validity of the diffusion mechanism for mouse movement has also been subjected to study. It has lead naturally to other spatial characteristics of mice behavior, such as the existence of home ranges [13, 14]. The analysis performed in those works, based on field data obtained for several Hantavirus related species of rodents, has led in turn to a new method for the determination of the typical home range size and diffusion coefficient, as a byproduct of field measurements of population densities [15].

Mean field models, simple as they are to write down, and relatively easy to analyze, are not satisfactory in the long run. They represent a *population level* description of the system. For fundamentally discrete and not very large populations, an *individual level* model is necessarily closer to the physical reality. Alas, as in all many-body problems, such microscopic approach is hopelessly unsolvable. Detailed numerical simulations are a possible alternative [5]. In the end, the microscopic level is also unsatisfactory. To bridge the gap, one needs a statistical description of the individual level, favoring some degree of generality in the depiction of the phenomena, and on the conclusions derived from them. One adequate tool for this level of description is the Master Equation, and approximate techniques of its analysis have already been used in the Hantavirus system [17] as well as in related ecological problems [18]. I will further report in this Chapter recent advances in the stochastic modelling of the Hantavirus-rodent system. I will show how to model these processes from the bottom up, in the form of a Master Equation. By means of an expansion of it, I will analyze the relation between the stochastic behavior and the mean field solutions. Several purely stochastic phenomena are of interest, such as the extinction of the epidemic by fluctuations. Furthermore, in related systems there are regimes in which the prevalence displays sustained oscillations, in spite of the fact that the mean field equations do not allow them. I will review also recent results pertaining the characterization of these oscillations.

## 2 Basic mean field: one species, no movement

We begin with a basic model, consisting of a single mouse species and no spatial extension. Also disregarded are sex and age. We keep the model intentionally simple to grasp the understanding of the basic mechanisms involved, while at the same time we incorporate as many facts about the ecology and epidemiology of the Hantavirus-mouse association as possible. We consider the total population divided into two categories: susceptible and infected (also infectious) mice. For these subpopulations, we propose a Susceptible-Infected (SI) model, as is standard for these systems (see, for example, [19] or [20]). This is a *mean*

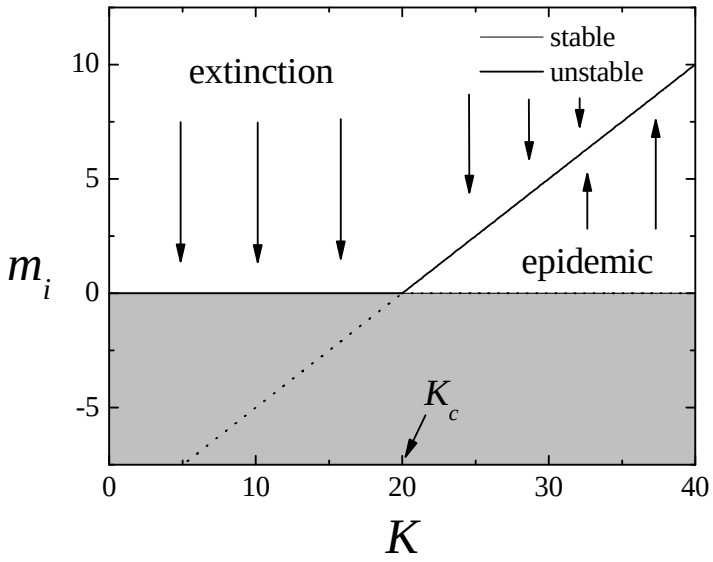


Figure 1: Bifurcation diagram of the basic model. The infected population is shown as a function of the carrying capacity $K$, which is used as a control parameter. There is a transcritical bifurcation at a value $K_c = b/[a(b-d)]$. The arrows show the direction of the flow for arbitrary initial conditions. The greyed region is unphysical (negative populations, unreachable from positive initial conditions).

*field*, or *well mixed* model, in which any mouse can interact with any other one (thus disregarding any spatial or correlation effect). The dynamics of the two subpopulations can be written as:

$$\frac{dm_s}{dt} = b\,m - d\,m_s - \frac{m_s m}{K} - a\,m_s m_i, \tag{1a}$$

$$\frac{dm_i}{dt} = -d\,m_i - \frac{m_i m}{K} + a\,m_s m_i, \tag{1b}$$

where $m_s$ and $m_i$ are the populations (or densities) of susceptible and infected mice, respectively, and $m(t) = m_s(t) + m_i(t)$ is the total population of mice. The motivation for the terms in Eqs. (1) follows.

*Births:* $b\,m$ represents births of mice, all of them born susceptible, at a rate proportional to the total density, since all mice contribute equally to the procreation [9].

*Deaths:* $d$ represents the rate of population decay by death, proportional to the corresponding density. If necessary, separate rates $d_s$ and $d_i$ could be introduced for the susceptible and infected populations respectively. For Hantavirus, which does not seem to alter any physiological parameter of their hosts, we have the same death rate for both susceptible and infected mice.

*Competition:* $-m_{s,i}m/K$ represent a limitation process in the population growth, due to competition for shared resources. Each is proportional to the probability of an encounter of a pair formed by one mouse of the corresponding class, susceptible or infected, and one mouse of any class (since every mouse, either susceptible or infected, has to compete

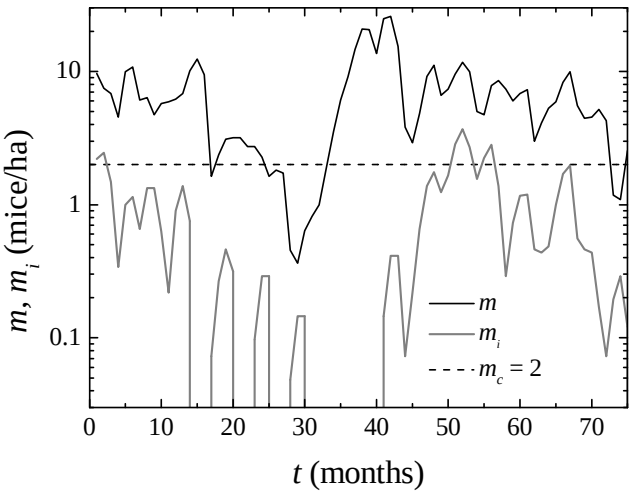


Figure 2: Mean density of *P. maniculatus* at two sites near Zuni, New Mexico, USA [after [12], Fig. 7]. Displayed: total population (back), infected with Sin Nombre Virus (grey), critical density (dashed). The time axis counts months from December 1994.

with the whole population). $K$ is a "carrying capacity," characterizing in a simplified way the capacity of the medium to maintain a population of mice. Higher values of carrying capacity represent a higher availability of water, food, shelter and other resources that mice can use to thrive [19].

*Contagion:* $a\, m_i m_s$ represents the number of susceptible mice that get infected, due to an encounter with an infected (and consequently infectious) mouse, at a rate $a$ that we assume constant. Contagion between deer mice is believed to take place during direct animal contact, mainly by biting (but see also [21] and [22] for different observations in related Hantaviruses). More elaborate models could incorporate a density dependence on $a$, for example due to an increased frequency of fights when the density is too high and the population feels overcrowded [10]. Since the infection is chronic, infected mice do not die of it, and infected mice do not lose their infectiousness probably for their whole life [9, 23], this single term adequately describes the infection dynamics of the two subpopulations.

Model (1) is able to successfully explain several field observations as environmentally controlled phase transitions, thus providing an analytical support to biological hypotheses such as the trophic cascade discussed in [12]. As shown in Figure 1, there is a critical value of the carrying capacity that separates two distinct regimes: if the environmental parameter $K$ is smaller than $K_c$, the stable equilibrium of $m_i$ is zero and infection is driven to extinction. If $K > K_c$, the infection may persist. In any real situation, where environmental conditions change as time goes by, the system can be expected to undergo transitions from one state to the other. This corresponds to the documented sporadic disappearance of the infection, as shown in Figure 2. (Notice that the populations are displayed in a logarithmic scale to emphasize the dynamics for low density values.) Total and infected densities are

shown, as indicated in the legend. Approximate demographic parameters can be obtained from the time series (details of the calculation can be found in [4]). From them, a critical population (related to the critical carrying capacity) can be derived, which is represented in the plot as a dashed line. This is the minimum population able to sustain a positive prevalence of infection, as predicted by the model defined by Eqs. (1). The prevalence of the infection is seen to decrease as soon as the population becomes subcritical,around $t = 15$. Eventually, the infection returns when the total population is supercritical again, but after a delay, just as expected from the model. After $t = 40$ the prevalence remains positive, as the population remains well above the critical value. The correlation between environmental patterns and human cases of Hantavirus Pulmonary Syndrome have been analyzed in [24]. The existence of a threshold in the population density in order to sustain a positive seroprevalence has directly been observed in another Hantavirus system, the Puumala virus in red bank voles in Belgium [8].

## 3 Waves of infection

Deer mice occupy most of North America, comprising a diverse landscape with a variety of habitats. Even local populations are subjected to the inhomogeneities of the landscape. These can be taken into account in a spatially extended version of the mean field model, where $m_s$, $m_i$ and $K$ become functions of a space variable $x$. The description of the dynamics now requires some assumption about mouse movements, i. e. a transport mechanism for the population. It is customary to assume a simple diffusion model to this end [16], so we can write the extended model as the following reaction-diffusion system:

$$\frac{\partial m_s}{\partial t} = b\, m - d\, m_s - \frac{m_s m}{K(x)} - a\, m_s m_i + D\nabla^2 m_s, \tag{2a}$$

$$\frac{\partial m_i}{\partial t} = -d\, m_i - \frac{m_i m}{K(x)} + a\, m_s m_i + D\nabla^2 m_i. \tag{2b}$$

Once more, we make no distinction between susceptible and infected mice, this time concerning their diffusion coefficient $D$. The solution of the system (2), and even its stationary solution, may be impossible to find, analytically, for an arbitrary function $K(x)$. Interesting situations correspond to a $K(x)$ that mimics the available resources in the landscape, such as the plant cover. Such maps can be constructed from remote sensors data, and used to estimate the risk for the human population. Several such studies have already been done, see for example Refs. [25, 26, 27]. In such a map, spots that remain supercritical for all environmental conditions play the role of the "refugia," some of which have been identified by the biologists in the field. Only at these refugia the infection thrives, even though susceptible mice may continue their occupation of the whole landscape, albeit with a lower population.

How does infection spread from refugia? When the prevalence in part of the landscape has dropped to zero, its eventual recovery, when environmental conditions change, necessarily involves the interaction with a region already infected. The mechanism for this spread is provided by solutions of system (2) in the form of nonlinear waves. Some general properties of these can be found analytically in a homogeneous environment, in which $K$ does not

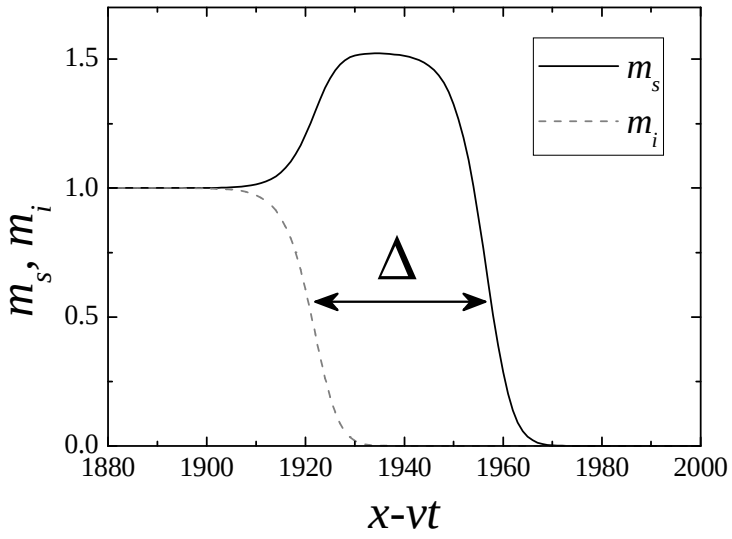


Figure 3: Front waves in the extended system, propagating from left to right. The populations are normalized to the equilibrium value. $a = 0.1$, $b = 1$, $d = 0.5$, $D = 1$, $K = 30.5$ ($K_0 = 30$).

depend on $x$. In such a case, as shown in [3], there can be invasion fronts consisting of a pair of waves, a leading one of susceptible mice, followed by a wave of infected ones. One such situation is illustrated in Figure 3. The speed of the susceptible front is the Fisher speed [19], $v_s = 2\sqrt{D(b-d)}$, while the infected front travels at $v_i = 2\sqrt{D[-b + aK(b-d)]}$. The fact that the latter depends on $a$ and $K$ induces the existence of a new transition, a dynamical one this time, as a function of the parameter $K$. If $K < K_0 = (2b-d)/[a(b-d)]$, then $v_i < v_s$ and the infected front progressively lags more and more behind the susceptible one. On the contrary, if $K > K_0$, then $v_i = v_s$ asymptotically, and the delay between the two fronts is a fixed value. This delay, shown as $\Delta$ in Fig. 3, depends on $K$ as well. A general situation can be studied in Fig. 4, that shows the evolution of the delay between the leading population front and the lagging infection front, from an adequate initial condition. Five situations are shown, corresponding to five different values of the supercritical carrying capacity $K$. The lower of these, $K = 21$, is barely above $K_c$, and well below $K_0$. So, even though the spread of the infection is granted, it does so much slowly than the whole population, with a delay that grows asymptotically as $t$. The three cases $K = 29$, 30 and 31 show what happens around the dynamical critical value $K_0 = 30$. All carrying capacities $K > K_0$ guarantee that the infectious front propagates as fast as the population spreads. These phenomena may result of relevance for the control of the epizootic, or for the forecast of its risk.

## 4 The role of biodiversity

As we have seen in the previous Sections, the pressure exerted by the environment on the population can drive the infection to extinction. Both subpopulations suffer this pressure in

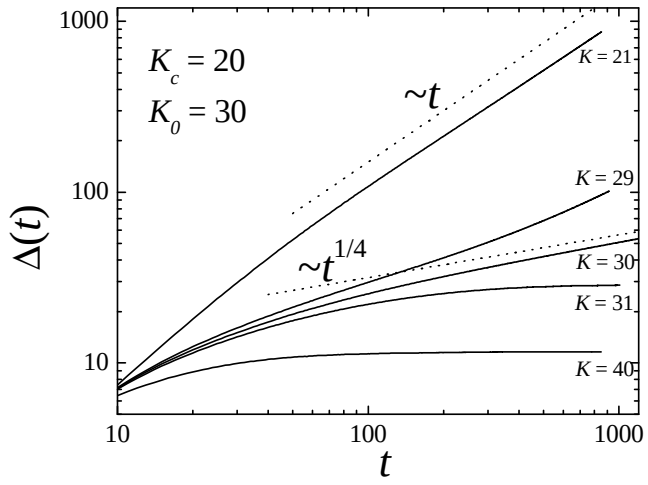


Figure 4: Evolution of the delay $\Delta$ between the susceptible front and the infection front (as shown in Figure 3). Different regimes are shown, corresponding to different values of $K > K_c$. Asymptotes $t$ and $t^{1/4}$, corresponding to the critical regimes, are shown in dashed lines.

the same way, but one of them, the infected, is more vulnerable, and becomes extinct at a finite value of $K$. The reason for this, certainly, is the lack of vertical transmission, peculiar to the Hantavirus. It is not difficult to imagine that other processes that limit the population size would play a similar role in the control of the infection. Among these processes a prominent role is played by the interaction with other species. In real ecosystems mice share the environment with many others species, competing for limited resources with some, and being preyed on by others.

The role of predation on the prevalence of a zoonotic disease has been analyzed by Ostfeld et al. in [28], and previously by Packer and others in [29]. Under the hypothesis that predation is the main factor in the interspecific relations of the species under consideration, they find that the incidence of the disease decreases with an increasing number of predators. The analysis relies on the fact that the population of predators is not affected by the population of prey—which allows to use them as a control parameter—a fact that can hold to a considerable degree if the predators are generalists. In small rodents populations such as the Hantavirus hosts, this is the case to a considerable extent.

A competitor species, on the other hand, is always affected by the competition if the shared resources are limited. The feedback on the host population, then, needs to be incorporated into the mathematical model. An initial step into the study of the effect of biodiversity on the prevalence of the infection can be found in [6]. There, a model is studied that consists of a single non-host population, competing with the host. This is a common situation in Hantavirus-mice systems [33]. On occasions, “alternative host” species have been observed, which are able to host the virus but for some reason are unable to trans-

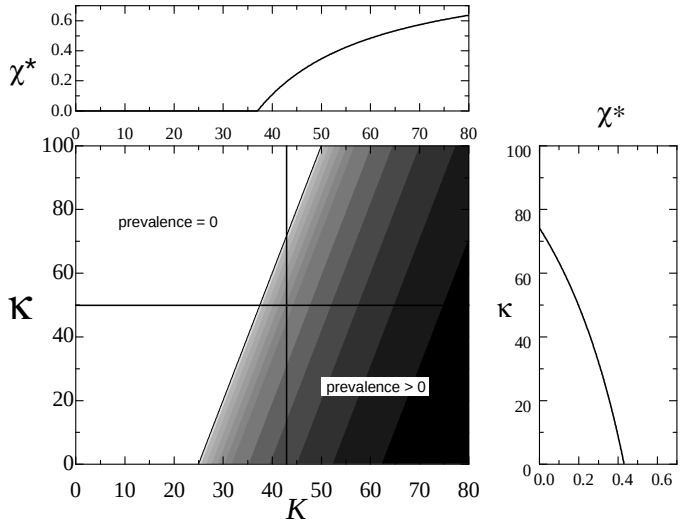


Figure 5: Phase diagram of the competition model. The infection prevalence $\chi = m_i/m$, is plotted in the space defined by carrying capacities, host ($K$) and non-host ($\kappa$). The contour plot shows the prevalence as shades of grey, with white being the region free of infection. The crossing lines indicate sections of the plot, shown in the upper and right side plots, where the prevalence is shown as a function of the relevant control parameter. The right panel represents the extinction of the infection controlled by the non-hosts carrying capacity.

mit it successfully. These, as well as non-host animals (such as predators or humans, for example) that come into contact with infected hosts, represent dead ends for the virus, but exercise an influence on the environment and an ecological pressure on the host, eventually affecting the dynamics of the epizootic. It is worth mentioning that biodiversity can result affected by numerous human activities, mainly by habitat destruction and fragmentation. These activities can have, as a mediate consequence, the increase of prevalence of zoonotic diseases.

Identifying the hosts by the variables $m_{s,i}$, and the non-host by $z$, the competition dynamics is the following:

$$\frac{dm_s}{dt} = b\,m - d\,m_s - \frac{m_s}{K}(m + qz) - a\,m_s m_i, \tag{3a}$$

$$\frac{dm_i}{dt} = -d\,m_i - \frac{m_i}{K}(m + qz) + a\,m_s m_i, \tag{3b}$$

$$\frac{dz}{dt} = (\beta - \delta)z - \frac{z}{\kappa}(z + \epsilon\,m), \tag{3c}$$

where, for the host species, $b$ is the birth rate, $d$ is the death rate, $K$ is the carrying capacity in the absence of a competing population ($z = 0$), and $q$ is the influence of the non-host population; for the non-host species, the analogous parameters are $\beta$, $\delta$, $\kappa$ and $\epsilon$ respectively.

The analysis of the equilibria of Eqs. (3) and their stability shows that competition reduces, in a specific way, the prevalence of the infection. Interestingly, this is in agreement

with (and provides theoretical support to) a hypothesis that was put to experimental test by G. Suzán in populations of *Z. brevicauda*, the host of the Calabazo Hantavirus, in field studies in Panama [34, 35]. There, a series of trapping sites were set up and observed during a period of 6 months, in a tropical region characterized by a high degree of biodiversity including several species of non-host competitors. One half of the sites were kept as controls, while in the other half biodiversity was drastically reduced, by removing all rodents but those belonging to the host species. An increase of seroconversion and seroprevalence was observed in the sites with reduced diversity. Similarly, also in Panama, it has been proposed that the maintenance of competitive populations may serve to reduce the risk to human populations exposed to *O. fulvescens* infected with the Choclo Hantavirus.[1] The proposal which has been called a "moat" consists of an area surrounding human habitation maintaining a diversity of innocuous species, competing with the hosts of the Hantavirus.

Figure 5 summarizes the behavior of system (3) in the form of a phase diagram. This representation generalizes Fig. 1 with the addition of the carrying capacity of the non-hosts, $\kappa$. It can be seen that a critical $\kappa$ drives the system to the noninfected state. Observe also that the "strength" of the competition with the non-host population, $q$, is the same for both susceptible and infected hosts. Indeed, both subpopulations are reduced as a result of the competition, but the infected population suffers the consequences in a stronger manner, becoming extinct in a critical way (see [6] for a discussion of this effect).

If an outbreak occurs at time $t = 0$ in the host population, one can calculate the determination of the critical value of the non-host population, necessary to suppress the spread of the epidemic:

$$z(0) = \frac{K[a\, m_s(0) - d] - m(0)}{q}, \tag{4}$$

where all the densities are evaluated at the initial time, $t = 0$, of the outbreak.

## 5 Mouse transport

Crucial for the quantitative application of the models reviewed in the previous Sections is the assignment of numerical values to the involved parameters. Let us consider again Eqs. (2). There are several parameters in these equations, not all of them equally accessible to observation. On the one hand, the demographic parameters, $b$ and $d$, are relatively easy to estimate from population data. On the other hand, the environmental parameter $K$ can be obtained, at least in relative values, from satellite images or other remote sensing of the landscape. The contagion parameter $a$, unfortunately, has proven to be extremely difficult to measure, even in controlled experiments (which are particularly difficult because of the high levels of biosafety required) [36]. Finally, there is $D$, the diffusion coefficient, of which not only its value is unknown, but even the validity of diffusion as mechanism for mice movement is to be asserted.

In a number of articles that rely heavily on the already mentioned field work carried on in Panama [34], and over one decade in New Mexico [37], this matter has been addressed by us [14, 13, 15]. The task provided, besides the possibility of the determination of the numerical value of the diffusivity of the species of our interest, with an opportunity to assess

[1] Koster, F., Lovelace Sandía Health System, personal communication (2004).

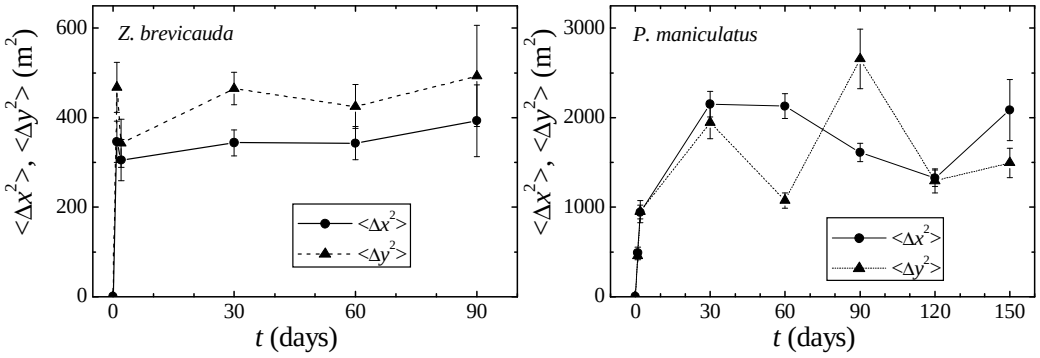


Figure 6: Mean square displacement as a function of time, from the two field works mentioned in the text (Panama, left panel, and New Mexico, right).

the validity of the diffusive transport, which sometimes is used for the lack of a better model, but which does not necessarily reflects the reality of the underlying animal phenomena. It is generally assumed that diffusive motion is an approximation, valid at some space and time scales, arising from a more complex "density dependent dispersion" (see the discussions in [16]). Interestingly, the analysis paved the way for a novel method for the determination of transport parameters from population measurements [15], of wider application than that of the Hantavirus epizootic.

Supposing independence of the captures, and homogeneity in the population, individual displacements were treated as an ensemble.[2] From this, curves representing the mean square displacement of the mice as a function of time were produced. These curves, shown in Fig. 6, immediately indicate that, while the movement is initially diffusive, it saturates very fast to an asymptotic value, as if the animals were bound to equilibrium positions, like the atoms in a crystal. This is a reminder of the complexities of the underlying system: the objects we are describing do not move like free diffusing particles. They are mice, of diverse sexes, ages and correspondingly, behavior. As in most mammals, it is characteristic of adult mouse movement the existence of a home range, where it passes the majority of its adult life. The saturation of the mean square displacement observed in Fig. 6 comes, in part, from the finite size of the home range. Besides the finite home range, the finiteness of the capture grid used in the field work also contributes to the same saturation. Both effects need to be taken into consideration in the statistical model, for the correct assessment of the curves of Fig. 6.

Since the mice do not move as free diffusing particles, one can do better by modelling a diffusive motion within a potential. The analysis can be carried out by describing the movement in terms of a Fokker-Planck Equation, which is a diffusion equation in a constraining potential (see [30, 31] for very detailed accounts). An illustration of the idea is shown in Fig. 7. Its mathematical formulation is:

$$\frac{\partial P(x,t)}{\partial t} = \frac{\partial}{\partial x}\left[\frac{dU(x)}{dx}P(x,t)\right] + D\nabla^2 P(x,t), \tag{5}$$

[2] A few animals were captured about 10 times during the study, allowing to picture, to some degree, the shape of their movements. A statistical analysis of them was, however, precluded by their small number.

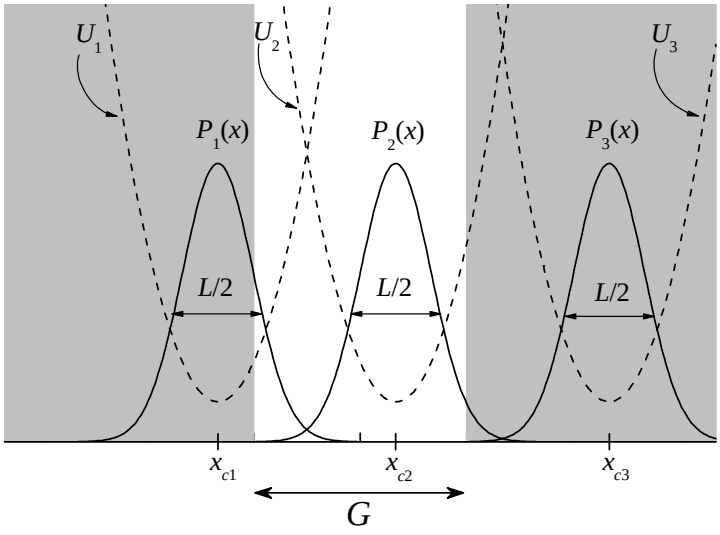


Figure 7: Illustration of the Fokker-Planck transport model. Three mice are shown, described by the probability density functions $P_i(x)$, each one living and diffusing within one of the potentials $U_i$. The central region, of width $G$, is the space accessible to observation, while the grey region is beyond reach of the capture grid.

where $P(x,t)$ is the probability density function of the occupation of space by an animal (its stationary state is typically a single peaked bell-shaped function). The function $U(x)$ is an abstract representation of the shape of the home range. Typically, it will be a concave function with a single minimum representing, for example, the position of the burrow. Once a shape is given to the "potential" $U$ (e. g. the parabolas used in Fig. 7), it is possible to calculate the mean square displacement from Eq. (5). In some cases, this can be done analytically. The calculation involves an average of the mean square displacement with probability distribution $P$, *restricted to the observation window*:

$$\langle \Delta x^2(t) \rangle = \frac{\int_{-G/2}^{G/2} (x - x_0)^2 P_{x_0}(x,t) dx}{\int_{-G/2}^{G/2} P_{x_0}(x,t) dx}, \tag{6}$$

where $x_0$ is the initial position of the animal. Additional averages are necessary: over these initial positions $x_0$, and over the distribution of the burrows (the centers of the parabolas in Fig. 7). We refer the interested reader to [15] for details of the calculation.

The diffusion coefficient follows, naturally, from the short time behavior of the mean square displacement. The long time behavior—the saturation—on the other hand, gives information about the shape of $U$, or the home range size, and can be contrasted with the saturation value of observed displacements such as those shown in Fig. 6. This is effectively, then, a method for calculating the (average) home range when no other observations (radio tracking of individuals, etc.) are available.[3] Indeed, it was developed as a by-product of field

[3]Borrowing terminology from fluid mechanics, it is like an Eulerian viewpoint as opposed to a Lagrangian one.

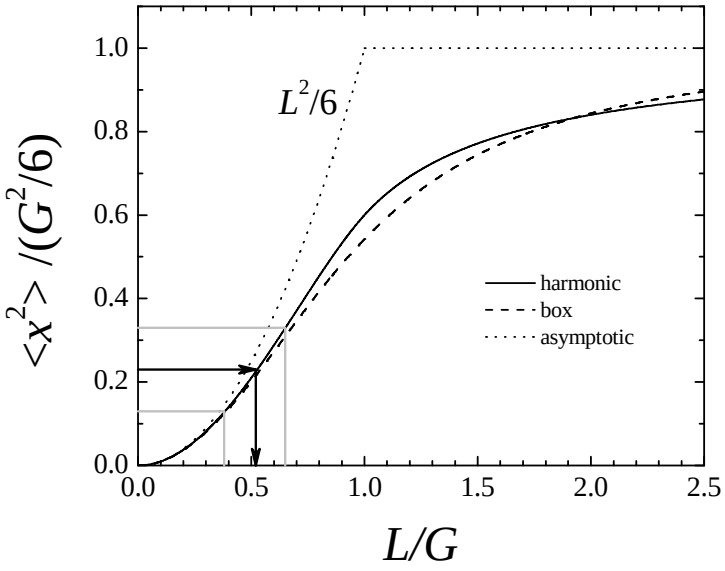


Figure 8: Stationary state of the mean square displacement, as a function of the ratio of the home range size to the grid size. Several possible potentials are shown. The arrows show the estimation of the home range size from the saturation values of the curves in Fig. 6.

work devised for the measurement of the population density. Figure 8 shows an example of such a calculation. Several curves are shown, corresponding to different chooses of the potential $U(x)$. It can be seen that they give essentially the same results, which is good, since the potential $U$ is not a physical object, and it is only a crude proxy for the way in which an average mouse occupies its home range. The saturation of the mean square displacement from the New Mexico observation is shown as an arrow in the ordinate axis, from which the ratio between the home range length and the (known) grid length, is read in the abscissas.

# 6 Bridging the gap between the mean field and individual based models

As mentioned in the Introduction, several facts about epizootics in wild populations call for an individual based formulation of the models, at least as a complement to a "macroscopic" mean field description. The stochastic nature of the interactions and processes that take place at the individual level, as well as the relatively small populations that may exist, are the origin of an inherently fluctuating dynamics that can only be captured by a stochastic model.[4]

[4]Sometimes the expression *demographic stochasticity* is used to refer to the fluctuations appearing in this kind of models, in which the fluctuations arise from the discrete nature of the populations and from stochastic individual processes. Another kind of models deal with *environmental stochasticity*, in which a fluctuating external agent (for example, a random $K(t)$ in Eq. (1)) exerts its influence onto an otherwise smooth variable.

The formulation of a stochastic model is relatively straightforward once the "microscopic" processes have been identified. It amounts to writing down a Master Equation [31], i. e. an evolution equation for the probability distribution of the system. Even though it is always a linear equation, the Master Equation can rarely be solved exactly, and either an approximate method, or a numerical scheme, or a combination of both, needs to be used. Since the use of a Master Equation model is not as widespread as the use of mean field models in biological applications, the present section contains more technical details than the previous ones. It also contains some previously unpublished developments, that are worth explaining. It is also worth mentioning a thorough analysis of several epidemic models based on a stochastic formulation, done by Nåsell in [32].

An underlying idea in the formulation of an individual based model is that in some "macroscopic" limit of description, where the populations are large, and one-individual changes are smooth, both descriptions coincide. Since many times the mean field equations are written down naively, differences may be found due to microscopic processes that were not correctly modelled at the population level. It is possible (at least in principle) to tailor a microscopic model which *a priori* would give a certain mean field model as a macroscopic limit. For the Hantavirus model of the previous sections, this has been done in [17]. In this section, we prefer to build the stochastic model from the bottom up. As I will show, there are differences that show up following this route.

## 6.1 Formulation of the stochastic model

Let us consider a population, composed of $S$ susceptible and $I$ infected animals, that dwell in a region of volume (area) $\Omega$. The animals are born, reproduce, and die according to certain rules, which are a simplification of the corresponding processes in a natural population. Within their habitat the animals compete for limited resources, as a result of which their populations become self-regulated. It is usual to distinguish two kinds of this intra-specific competition: indirect, by exploitation of a finite resource, and direct, by interference between pairs of animals (see for example the treatise by Begon [38]). We will incorporate both mechanisms into the stochastic model, as follows. Indirect competition will be supposed to limit the reproduction of animals by affecting a necessary resource for reproduction to take place. Following McKane [18], let us represent this resource as an additional population, $E$, related to the volume and the animals populations by:

$$E = q\Omega - S - I, \tag{7}$$

where $q$ is a parameter that measures the carrying capacity of the environment.[5] $E$ can be thought of as *available slots* in the community: if $S$ and $I$ are such that, given $q$ and $\Omega$, $E = 0$, there is no possibility of further reproduction. McKane has shown, in [18], that the indirect interaction between individuals of a single population, provided by the resources population $E$, gives exactly the expected logistic equation in the macroscopic limit. We will refer to $E$, informally, as the "empty population," or the "empty space" of the system. With the help of the population $E$ we can write the following "reactions" that characterize the demographic processes. The parameters written above the arrows represent the rates

[5] $1 - q$ is analogous to the *destruction of the habitat*, $D$, in Tilman's model [39].

at which the processes occur (the nomenclature has been kept similar to the mean field models.[6])
Birth (limited by indirect competition):

$$\text{birth to susceptible:} \quad S + E \xrightarrow{b_s} S + S \tag{8a}$$

$$\text{birth to infected:} \quad I + E \xrightarrow{b_{is}} I + S \tag{8b}$$

$$\text{birth to infected:} \quad I + E \xrightarrow{b_{ii}} I + I \tag{8c}$$

Death:

$$\text{death of susceptible:} \quad S \xrightarrow{d_s} E \tag{9a}$$

$$\text{death of infected:} \quad I \xrightarrow{d_i} E \tag{9b}$$

Death by direct competition:

$$S + S \xrightarrow{1/K} S + E \tag{10a}$$

$$I + I \xrightarrow{1/K} I + E \tag{10b}$$

$$S + I \xrightarrow{1/(2K)} S + E \tag{10c}$$

$$S + I \xrightarrow{1/(2K)} I + E \tag{10d}$$

Contagion:

$$S + I \xrightarrow{r} I + I \tag{11}$$

The reactions (8) show the self-limiting effect of indirect competition: a slot $E$ is necessary for a birth event to take place and, through (7), the $E$'s are depleted by the animals present in the system. Deaths, either "natural" (9) or as the result of direct competition (10), replenish the available resources.

Observe, also, that some of these reactions represent alternative outcomes of the same pair of interacting units. For example, the reproduction of an infected animal can produce either a susceptible or an infected one, with this last case referred to as *vertical transmission*. Similarly, the direct interaction of a susceptible and an infected in Eq. (10) can result in the death of the former or of the latter. The reaction rates, in these cases, must satisfy some constraints, as represented by the additional factor $1/2$ in the latter.

The state of the system at any time is described by the multivariate probability density function $P(S, I, t)$, of the stochastic variables $S$ and $I$. The Master Equation is a gain-lose equation for $P(S, I, t)$. It reads, in general:

$$\frac{dP(S,I)}{dt} = \sum_{j,k} T(S, I|S_j, I_k)P(S_j, I_k) - \sum_{j,k} T(S_j, I_k|S, I)P(S, I), \tag{12}$$

where the sum is taken over all the states that have allowed transitions to or from the state $(S, I)$. The notation for the transition probabilities, $T(Y|X)$, means that the system goes from state $X$ to state $Y$ with a probability $T$ per unit time.

[6]The contagion rate has been changed to $r$ because of a technical detail that forces $a$ to be $2r$.

Transitions between different states are provided by the processes (8-11). To proceed, one must calculate the transition probabilities for all the allowed processes, taking into account the rates as well as the probability of encounter of the participating pairs. Let us write down these transition probabilities for the processes that *start* at a state $(S, I)$. There are corresponding ones for transitions *ending* at the state $(S, I)$, which can also be written down without difficulty, but we will not need them in the following:

$$T(S+1, I|S, I) = 2b_s \frac{S}{\Omega}\frac{E}{\Omega - 1} + 2b_{is}\frac{I}{\Omega}\frac{E}{\Omega - 1} \tag{13a}$$

$$T(S, I+1|S, I) = 2b_{ii}\frac{I}{\Omega}\frac{E}{\Omega - 1} \tag{13b}$$

$$T(S-1, I|S, I) = d_s\frac{S}{\Omega} + \frac{1}{K}\frac{S}{\Omega}\frac{S-1}{\Omega - 1} + 2\frac{1}{2K}\frac{S}{\Omega}\frac{I}{\Omega - 1} \tag{14a}$$

$$T(S, I-1|S, I) = d_i\frac{I}{\Omega} + \frac{1}{K}\frac{I}{\Omega}\frac{I-1}{\Omega - 1} + 2\frac{1}{2K}\frac{S}{\Omega}\frac{I}{\Omega - 1} \tag{14b}$$

$$T(S-1, I+1|S, I) = 2r\frac{S}{\Omega}\frac{I}{\Omega - 1} \tag{15}$$

Observe that, in these transition probabilities, the fractions $X/\Omega$—where $X$ is one of the subpopulations—correspond to the probabilities of picking the corresponding animal at random in the system. The fact that these probabilities depend only on the total subpopulation and the size of the system is a convenient simplification, which could eventually be relaxed to take into account spatial distribution or clustering of individuals. In this sense, this stochastic model is already a mean field model. Observe also that there is a factor 2 in the probabilities of the processes that involve two elements of different populations, such as $S+I$, which is not present in single animal events (deaths) or in events that involve animals of the same population. In this, we are considering that the animals within a population are indistinguishable, effectively as molecules in a chemical system.

The form of the Master Equation becomes more manageable in terms of the following *step operators*, defined through their action on the state variables [31]:

$$\epsilon_s f(S) = f(S+1), \tag{16a}$$

$$\epsilon_i f(I) = f(I+1), \tag{16b}$$

and their inverses:

$$\epsilon_s^{-1} f(S) = f(S-1), \tag{16c}$$

$$\epsilon_i^{-1} f(I) = f(I-1). \tag{16d}$$

With these operators, one can write an expression only involving transition probabilities

that start at $(S, I)$:

$$\begin{aligned}\frac{dP(S,I)}{dt} =&(\epsilon_s - 1)T(S-1, I|S, I)P(S, I)\\ &+ (\epsilon_i - 1)T(S, I-1|S, I)P(S, I)\\ &+ (\epsilon_s^{-1} - 1)T(S+1, I|S, I)P(S, I)\\ &+ (\epsilon_i^{-1} - 1)T(S+1, I|S, I)P(S, I)\\ &+ (\epsilon_s\epsilon_i^{-1} - 1)T(S-1, I+1|S, I)P(S, I).\end{aligned} \tag{17}$$

## 6.2 Expansion of the Master Equation

The systematic expansion of the Master Equation devised by van Kampen [31] relies on the following ansatz, that decomposes each stochastic variable into a macroscopic, analytical one, plus a noise of smaller amplitude:

$$S(t) = \Omega\phi(t) + \sqrt{\Omega}\xi(t), \tag{18a}$$
$$I(t) = \Omega\psi(t) + \sqrt{\Omega}\eta(t). \tag{18b}$$

This is a very reasonable assumption, which results justified *a posteriori* for stable systems. It should be understood that the stochastic variables $S$ and $I$, during their time evolution, will be characterized by certain bell-shaped distributions, whose peaks will move smoothly following the intensive variables $\phi(t)$ and $\psi(t)$, and whose widths will be $\sqrt{\Omega}$ smaller when compared with their averages.

The step operators were introduced above because they have simple expansions in powers of $\sqrt{\Omega}$. For example:

$$\epsilon_s = 1 + \frac{1}{\sqrt{\Omega}}\frac{\partial}{\partial\xi} + \cdots \tag{19a}$$
$$\epsilon_s^{-1} = 1 - \frac{1}{\sqrt{\Omega}}\frac{\partial}{\partial\xi} + \cdots, \tag{19b}$$

and similarly for $\epsilon_i$.

The use of Eqs. (18) and (19) in the Master Equation (17) provides an expansion in powers of $\Omega^{-1/2}$ that can be analyzed order by order. The procedure has several advantages. The principal one is that it is systematic, and that it is an expansion in terms of a small parameter. If the system is stable, the expansion can be cut wherever it is convenient. Let us give just one example of them, supposing that only *indirect* competition is at play, and that the demographic processes are those of the Hantavirus infection: $b_s = b_{is} \equiv b$, $b_{ii} = 0$ (no vertical transmission), $d_s = d_i \equiv d$ (no additional death rate for infected animals), and $q = 1$.[7] The following expression shows the first terms of the expansion of the Master Equation, where we have called $\Pi(\xi, \eta, t)$ the probability distribution $P(S, I, t)$, through

[7] As it is also usual, the rates have been scaled with a factor $1/(\Omega - 1)$ in the expressions that follow, even though no change of notation has been made, to reduce the clutter of the expressions. See, for example, [18], where a similar calculation is carried out in great detail.

the dependence of $S$ and $I$ on the stochastic fluctuations $\xi$ and $\eta$:

$$\begin{aligned}
&\frac{\partial \Pi}{\partial t} - \sqrt{\Omega}\left(\frac{d\phi}{dt}\frac{\partial \Pi}{\partial \xi} + \frac{d\psi}{dt}\frac{\partial \Pi}{\partial \eta}\right) = \\
&\quad d\left(\frac{1}{\sqrt{\Omega}}\partial_\xi + \frac{1}{2\Omega}\partial_{\xi\xi}\right)\left(\Omega\phi + \sqrt{\Omega}\xi\right)\Pi + \\
&\quad d\left(\frac{1}{\sqrt{\Omega}}\partial_\eta + \frac{1}{2\Omega}\partial_{\eta\eta}\right)\left(\Omega\psi + \sqrt{\Omega}\eta\right)\Pi + \\
&\quad 2b\left(-\sqrt{\Omega}\partial_\xi + \frac{1}{2}\partial_{\xi\xi}\right)\left(1 - \phi - \psi - \frac{1}{\sqrt{\Omega}}\xi - \frac{1}{\sqrt{\Omega}}\eta\right)\left(\phi + \psi + \frac{1}{\sqrt{\Omega}}\xi + \frac{1}{\sqrt{\Omega}}\eta\right)\Pi + \\
&\quad 2r\left[\sqrt{\Omega}(\partial_\xi - \partial_\eta) + \frac{1}{2}(\partial_{\xi\xi} - \partial_{\xi\eta} + \partial_{\eta\eta})\right]\left(\phi + \frac{1}{\sqrt{\Omega}}\xi\right)\left(\psi + \frac{1}{\sqrt{\Omega}}\eta\right)\Pi \\
&\quad + O(\sqrt{\Omega}^{-1}).
\end{aligned} \tag{20}$$

### 6.3 Macroscopic equations

The leading order in Eq. (20) is that of $\sqrt{\Omega}$. This needs to be made null, in order that the expansion behaves regularly when $\Omega \to \infty$. Equating both sides of this order, and given that fluctuations in $\xi$ and $\eta$ are independent, we arrive at the following set of two ordinary differential equations for the intensive variables:

$$\frac{d\phi}{dt} = -d\,\phi + 2b(\phi + \psi)(1 - \phi - \psi) - 2r\,\phi\psi, \tag{21a}$$

$$\frac{d\psi}{dt} = -d\,\psi + 2r\,\phi\psi. \tag{21b}$$

These are the equations of the mean field, macroscopic level of description. They give the dynamics of the smooth population variables that can be observed, for example, averaging over realizations in a numerical simulation of the system.

Compare these equations with Eqs. (1). The main difference is the lack of a saturation term in the equation for the infected. The reason is that we modelled only *indirect* competition (births mediated by available resources) in (21). Equation (1), one realizes, corresponds to *direct* competition only; it can be obtained exactly as the macroscopic behavior of the stochastic model, by taking the transitions (10) into account. It should be noted that a real system would be better modelled by including both kinds of competition.

Despite this difference in the nature of the self-limiting term, typical bifurcation diagrams of the equilibrium solutions of Eqs. (21) look very similar to those of Eqs. (1). As Fig. 9 shows, there is also a transcritical bifurcation. The left panel shows the effect of different birth rates. It includes curves corresponding to two values of $q$, showing that the lower ones affect strongly the infected population. The right panel shows the bifurcation as a function of $q$. It is seen that less available habitat affects the infected to a greater degree than the susceptible, just as the carrying capacity $K$ did in the mean field model of Section 1.

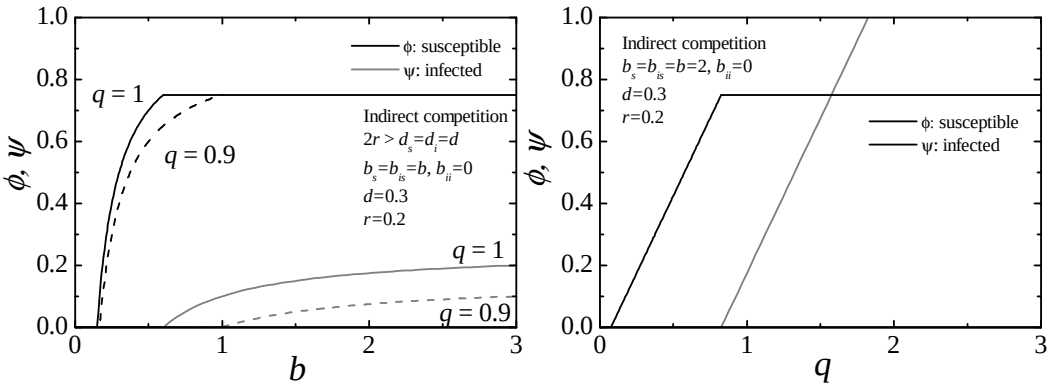


Figure 9: Susceptible and infected densities for the indirect competition microscopic model. Left: as a function of the birth rate; curves are shown for two values of $q$. Right: as a function of $q$; this bifurcation diagram can be compared with the mean-field model (direct competition) of Fig. 1.

## 6.4 Fluctuations

The following order in the expansion, found by equating the terms of order $\Omega^0$, represents the main behavior of the deviations from the macroscopic variables. It takes the form of a linear Fokker-Planck equation for the probability distribution function of the fluctuations $\xi$ and $\eta$. For the indirect competition model and the same parameters restriction as used in Eq. (20), this evolution equation for the distribution of fluctuations reads:

$$\begin{aligned}\frac{\partial \Pi(\xi,\eta,t)}{\partial t} =& -a_{11}\frac{\partial}{\partial \xi}\xi\Pi(\xi,\eta,t) - a_{12}\frac{\partial}{\partial \xi}\eta\Pi(\xi,\eta,t) \\ & - a_{21}\frac{\partial}{\partial \eta}\xi\Pi(\xi,\eta,t) - a_{22}\frac{\partial}{\partial \eta}\eta\Pi(\xi,\eta,t) \\ & + \frac{1}{2}\left[b_{11}\frac{\partial^2}{\partial \xi^2}\Pi(\xi,\eta,t) + (b_{12}+b_{21})\frac{\partial^2}{\partial \xi \partial \eta}\Pi(\xi,\eta,t) + b_{22}\frac{\partial^2}{\partial \eta^2}\Pi(\xi,\eta,t)\right],\end{aligned} \tag{22}$$

where:

$$a_{11} = -d + 2b(1-2\phi-2\psi) - 2r\psi, \tag{23a}$$
$$a_{12} = 2b(1-2\phi-2\psi) - 2r\phi, \tag{23b}$$
$$a_{21} = 2r\psi, \tag{23c}$$
$$a_{22} = -d + 2r\phi, \tag{23d}$$

and

$$b_{11} = d\phi + 2b(\phi+\psi)(1-\phi-\psi) + 2r\psi, \tag{24a}$$
$$b_{12} = b_{21} = -r\phi\psi, \tag{24b}$$
$$b_{22} = d\psi + 2r\phi\psi. \tag{24c}$$

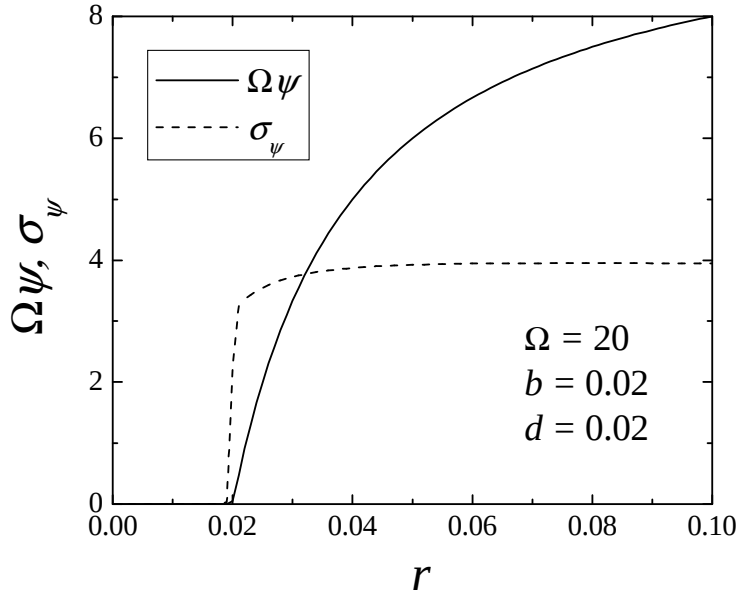


Figure 10: Average infected density $\psi$ and its standard deviation $\sigma_\psi$, for the indirect competition stochastic model.

Equation (22) is a linear Fokker-Planck equation, the solution of which is a Gaussian (for appropriate initial and boundary conditions). Observe that the coefficients of the equation depend on time through the functions $\phi(t)$, $\psi(t)$, that is, the solutions of the macroscopic law. Further orders in the expansion modify this Gaussian nature of the fluctuations, but one need not consider them in general. The next order, for example, is of order $\Omega^{-1}$ relative to the macroscopic values, and so of the order of a single animal.

Since the solution of Eq. (22) is a Gaussian, it is equivalent to seek for solutions of the equations governing the first two moments of $\xi$ and $\eta$. The time dependence of these comes through the time dependence of $\phi$ and $\psi$, solutions of Eq. (21), with appropriate initial conditions. This problem can be analytically solvable or not, but in any case it is always possible to find the fluctuations around the *steady state* $(\phi^*, \psi^*)$. Of particular interest is the calculation of the second moments of $\Pi(\xi, \eta, t)$, which can be compared to the variances of the fluctuations in simulations or field measurements (see [31] for a derivation of this from the Fokker-Planck equation):

$$\partial_t \langle \xi^2 \rangle = 2a_{11}\langle \xi^2 \rangle + 2a_{12}\langle \xi\eta \rangle + b_{11}, \tag{25a}$$

$$\partial_t \langle \xi\eta \rangle = a_{21}\langle \xi^2 \rangle + (a_{11} + a_{22})\langle \xi\eta \rangle + a_{12}\langle \eta^2 \rangle + b_{12}, \tag{25b}$$

$$\partial_t \langle \eta^2 \rangle = 2a_{21}\langle \xi\eta \rangle + 2a_{22}\langle \eta^2 \rangle + b_{22}, \tag{25c}$$

to be solved, together with Eqs. (21), with appropriate initial conditions such as the follow-

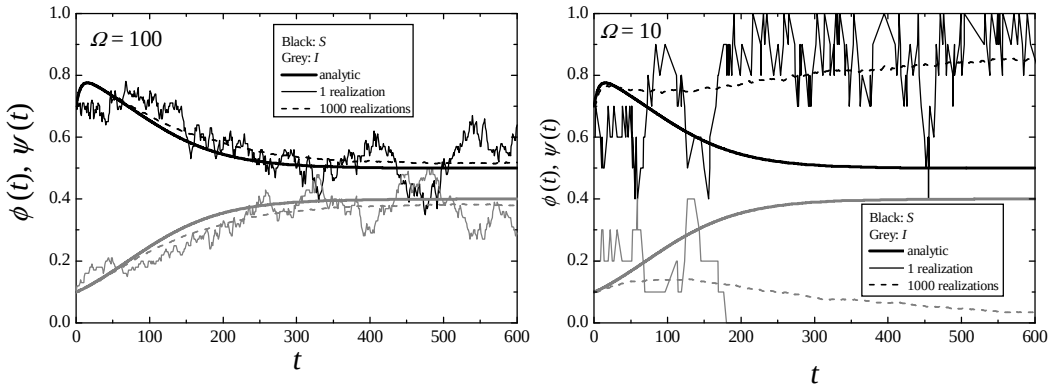


Figure 11: Comparison between numerical simulations of the indirect competition model, and the solution of the macroscopic equations. In both panels, the analytic solution is shown as a thick line. The narrower lines correspond to a single realization (jagged lines) and average of 1000 realizations (dashed lines).

ing ones:

$$\phi(0) = \phi_0, \tag{26a}$$

$$\psi(0) = \psi_0, \tag{26b}$$

$$\langle \xi^2 \rangle(0) = \langle \xi\eta \rangle(0) = \langle \eta^2 \rangle = 0, \tag{26c}$$

which imply that the initial distribution of $S$ and $I$ is a delta at $\phi_0, \psi_0$.

Figure 10 shows the stationary solution of Eqs. (21,25) as a bifurcation diagram with the contagion rate $r$ as a control parameter. The curves have been scaled to show the behavior of a (small) system of $\Omega = 20$. It can be seen that, for such a small system, the fluctuations are always big with respect to the means. It is seen, also, that this situation worsens when the system is close to the critical transition. This is the origin of the extinctions due to fluctuations in finite systems, a phenomenon that is not described by the mean field models.

## 6.5 Numerical simulations

The numerical simulation of a system defined by the reactions (8-11) can be implemented by the dynamical Monte Carlo method of Gillespie [41, 42], which is a direct implementation of the Master Equation. Figure 11 shows two instances of such simulations, corresponding to two different volumes (measured as $\Omega = 100$ and 10, in units of individual animal volume). Observe how the amplitude of the fluctuations is smaller for large systems, and that in the largest one the macroscopic equations give an rather good approximation of the stochastic system (for the same parameters and $\Omega = 10000$, the average of 100 realizations would be indistinguishable at this scale). Smaller systems, on the other hand, are not only more fluctuating, but also show a departure from the macroscopic behavior, showing the inherent limitation of the systematic expansion. Observe, also, that large fluctuations can lead one of the populations to extinction. Once extinct, the infected population cannot

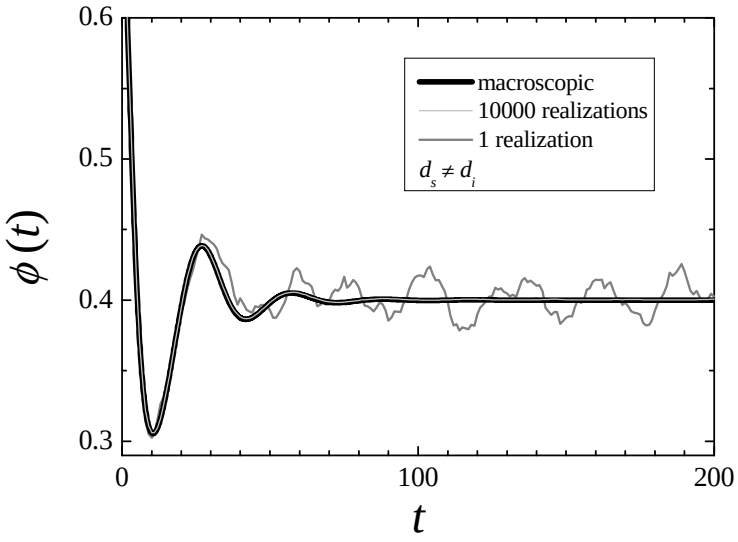


Figure 12: Comparison between numerical simulations of the indirect competition model, and the solution of the macroscopic equations. The macroscopic solutions display damped oscillations, and the average of many realizations coincide with them. Any single realization, however, shows persistent oscillations of a well defined frequency.

recover in this system, even though the corresponding equilibrium is unstable in the mean field model. The average time to extinction is, in principle, also a tractable problem in the linear noise approximation. A more general treatment has been done by Nåsell in [43].

### 6.6 Amplification of oscillations

The stabilization of oscillations is an interesting phenomenon displayed by certain stochastic models, whose macroscopic counterparts *do not oscillate*. These oscillations arise purely from fluctuations, by the collective synchronization of individual transitions through their interactions [44]. The amplitude of the oscillations tends to 0 as the system size tends to $\infty$ (indeed, as $\Omega^{-1/2}$), but for finite systems, these persistent oscillations may explain, or contribute to, the (non-seasonal) oscillations in many epidemiological and ecological systems (examples of these are analyzed in [45] or [46]). It has been shown by McKane [40] that this phenomenon resembles a resonance, to a certain degree. For the $SI$ system of the Hantavirus, as presented in this section, we have shown that sustained oscillations are not possible, since it is required that the two subpopulations are distinguishable: either with different death rates, or birth rates, etc. A modification in this sense, however, immediately shows this phenomenon. See Fig. 12 for an example in which $d_s \neq d_i$. The analytic curve (thick black line) shows just damped oscillations. So does the average of 10000 realizations that closely coincides with it (thin grey line, on top of the black one). The averaging of many individual realizations hides the oscillations, since they are not in phase from one realization to the next. A single realization, such as the one shown Fig. 12, however, clearly shows persistent oscillations.

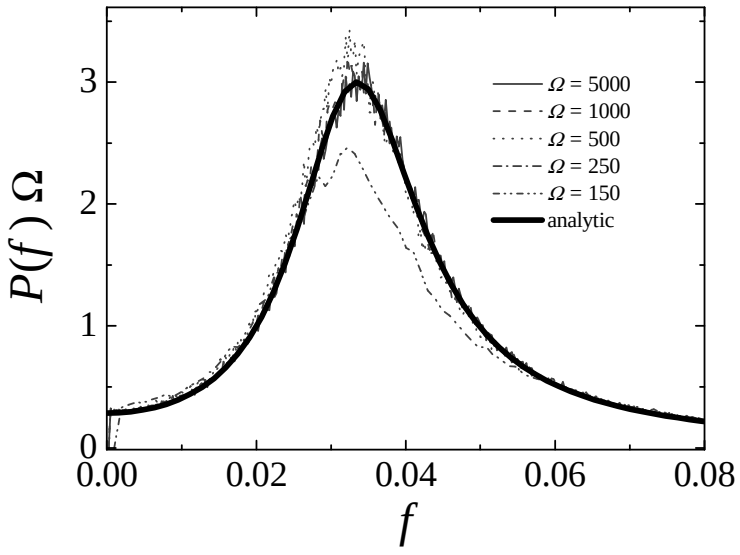


Figure 13: Spectrum of oscillations of the infected population. The analytical, approximate, result is compared to spectra obtained by FFT of simulations of varying system size.

The power spectrum of the oscillating populations can also be calculated within the framework of the van Kampen expansion, as shown also by McKane in [40]. The resulting curve compares well with the spectra calculated by Fast Fourier Transform of simulated populations, as shown in Fig. 13. Even for small systems a peak is seen, at nearly the same frequency. The correspondence between these spectra shows that the linear noise approximation in the van Kampen expansion is indeed a good one for these systems. We have developed a quantitative characterization of these "stochastic oscillations," based on the properties of the spectrum [47]. It allows an assessment of the quality of the oscillations (as contrasted with random noise) based on the parameters on the macroscopic equations. These matters fall beyond the scope of the present review, and we refer the interested reader to that work for the details.

## 7 Conclusion

We have reviewed simple models of infection in mice populations, able to capture the important effects of the Hantavirus epizootic as controlled by the environment. The models have been intentionally kept simple to allow a direct treatment of the consequences by analytical means.

Two levels of description were analyzed: a population level, and an individual level. The former, epitomized by mean field models, produces results in which several phenomena characteristic of the epizootic are observed. Some of them are in agreement with field observations, and others are predicted: the extinction and spatial segregation of the infected population, the propagation of delayed infection fronts, the reduction of the prevalence

by competition effect. We have also seen that relevant parameters of the system can be derived from limited data sets: the diffusion coefficient and the home range size. Even though mouse "transport" is more complex than diffusion, there is a certain possibility for analytical models to improve the analysis of the epizootic system.

The individual based level of description can be studied by numerical simulation and by approximate analytical developments. It has the advantage that fluctuations and their consequences can be formalized and analyzed. Among them, the characteristic deviations from the macroscopic values, extinctions due to fluctuations, and stabilization of oscillations.

Many features have been left outside of the analysis (such as the role played by different ages and sexes in the dynamics of the infection). The field continues to be active, and many of them are being, or will soon be incorporated into the standard body of knowledge.

## Acknowledgements

Along the years, I have enjoyed fruitful collaboration with my colleagues Nitant Kenkre, Ignacio Peixoto, Luca Giuggioli, Sebastián Risau-Gusman. Valuable has also been the interaction with the biologists from the University of New Mexico, from whom I learn a great deal about Hantaviruses and mice: Gerardo Suzán, Bob Parmenter, Terry Yates, Erika Marcé, Fred Koster, and many of their colleagues that I met in their Department. I acknowledge financial support from ANPCyT (PICT-R 02-87/2 and 04-943) and from CONICET (PIP 5114), and the hospitality of the Abdus Salam ICTP, where this chapter was written.

## References

[1] Mills, J. N. and Childs, J. E., *Ecologic Studies of Rodent Reservoirs: Their Relevance for Human Health*, Emerg. Inf. Diseases **4**, no. 4, 529-534 (1998).

[2] Abramson, G. and Kenkre, V.M., *Spatio-temporal patterns in the Hantavirus infection*, Phys. Rev. E **66**, 011912 (2002).

[3] Abramson, G., Kenkre, V.M., Yates, T.L. and Parmenter, B.R., *Traveling waves of infection in the Hantavirus epidemics*, Bull. Math. Biol. **65**, 519-534 (2003).

[4] Abramson, G., *The criticality of the Hantavirus infected phase at Zuni*, Electronic article arXiv:q-bio.PE/0407003 (2004).

[5] Aguirre, M.A., Abramson, G., Bishop, A.R. and Kenkre, V.M., *Simulations in the mathematical modeling of the spread of the Hantavirus*, Phys. Rev. E **66**, 041908 (2002).

[6] Peixoto, I. D. and Abramson, G., *The effect of biodiversity on the Hantavirus epizootic*, Ecology **87**, 873-879 (2006).

[7] Kenkre, V. M., Giuggioli, L., Abramson G. and Camelo-Neto, G. *Theory of Hantavirus infection spread incorporating localized adult and itinerant juvenile mice*, Eur. Phys. J. B **55**, 461-470 (2007).

[8] Escutenaire, S., Chalon, P., Verhagen, R., Heyman, P., Thomas, I., Karelle-Bui, L., Avsic-Zupanc, T., Lundkvist, A., Plyusnin A., and Pastoret, P.-P., *Spatial and temporal dynamics of Puumala hantavirus infection in red bank vole (*Clethrionomys glareolus*) populations in Belgium*, Virus Research **67**, 91-107 (2000).

[9] Mills, J. N., Ksiazek, T. G., Peters, C. J. and Childs, J. E., *Long-term studies of Hantavirus reservoir populations in the Southwestern United States: A synthesis*, Emerging Infectious Diseases **5**, 135 (1999).

[10] Calisher, C. H., Sweeney, W., Mills J. N. and Beaty, B. J., *Natural history of Sin Nombre virus in Western Colorado*, Emerging Infectious Diseases **5**, 126 (1999).

[11] Parmenter, C. A., Yates, T. L., Parmenter R. R. and Dunnum, J. L., *Statistical sensitivity for detection of spatial and temporal patterns in rodent population densities*, Emerging Infectious Diseases **5**, 118 (1999).

[12] Yates, T. L., Mills, J. N., Parmenter, C. A., Ksiazek, T. G., Parmenter, R. R., Vande Castle, J. R., Calisher, C. H., Nichol, S. T., Abbott, K. D., Young, J. C., Morrison, M. L., Beaty, B. J., Dunnum, J. L., Baker, R. J., Salazar-Bravo, J. and Peters, C. J., *The ecology and evolutionary history of an emergent disease*, Bioscience **52**, no. 11, 989-998 (2002).

[13] Giuggioli, L., Abramson, G., Kenkre, V. M., Suzán, G., Marcé E. and Yates, T. L., *Diffusion and home range parameters from rodent population measurements in Panama*, Bull. Math. Biol. **67**, 1135-1149 (2005).

[14] Abramson, G., Giuggioli, L., Kenkre, V. M., Dragoo, J. W., Parmenter, R. R., Parmenter, C. A. and Yates, T. L., *Diffusion and home range parameters for rodents II:* Peromyscus maniculatus *in New Mexico*, Ecological Complexity **3**, 64-70 (2006).

[15] Giuggioli, L., Abramson G. and Kenkre, V. M., *Theory of home range estimation from mark-recapture measurements of animal populations*, J. Theor. Biol. **240** 126-135 (2006).

[16] Okubo, A., *Diffusion and Ecological Problems: Modern Perspectives*, 2nd. edition. Springer-Verlag, Berlin (1980).

[17] Escudero, C., Buceta, J., de la Rubia, F. J. and Lindenberg, K., *Effects of internal fluctuations on the spreading of Hantavirus*, Phys. Rev. E **70**, 061907 (2004).

[18] McKane, A. J. and Newman, T. J., *Stochastic models in population biology and their deterministic analogs*, Phys. Rev. E **70**, 041902 (2004).

[19] Murray, J. D., *Mathematical Biology*, 2nd ed. Springer, New York, USA (1993).

[20] Anderson, R. M., May, R. M. and Anderson, B., *Infectious Diseases of Humans: Dynamics and Control*, Oxford Science Publications (1992).

[21] Orellana, C., *Chilean research throws light on hantavirus transmission*, The Lancet Inf. Dis. **3**, 8 (2003).

[22] Kallio, E. R., Klingström, J., Gustafsson, E., Manni, T., Vaheri, A., Henttonen, H., Vapalahti, O. and Lundkvist, Å., *Prolonged survival of Puumala hantavirus outside the host: evidence for indirect transmission via the environment*, J. Gen. Virology **87**, 2127-2134 (2006).

[23] Kuenzi, A. J., Morrison, M. L., Swann, D. E., Hardy, P. C. and Downard, G. T., *A longitudinal study of Sin Nombre virus prevalence in rodents, Southeastern Arizona*, Emerging Infectious Diseases **5**, 113 (1999).

[24] Engelthaler, D. M., Mosley, D. G., Cheek, J. E., Levy, C. E., Komatsu, K. K., Ettestad, P., Davis, T., Tanda, D. T., Miller, L., Frampton, J. W., Porter R. and Bryan, R. T., *Climatic and environmental patterns associated with Hantavirus Pulmonary Syndrome, Four Corners Region, United States*, Emerging Infectious Diseases **5**, 87-94 (1999).

[25] Boone, J. D., McGwire, K. C., Otteson, E. W., DeBaca, R. S., Kuhn, E. A., Villard, P., Brussard P. F. and St. Jeor, S. C., *Remote sensing and geographic information systems: Charting Sin Nombre virus infections in deer mice*, Emerging Infectious Diseases **6**, 248-258 (2000).

[26] Glass, G. E., Yates, T. L., Fine, J. B., Shields, T. M., Kendall, J. B., Hope, A. G., Parmenter, C. A., Peters, C. J., Ksiazek, T. G., Li, C.-S., Patz, J. A. and Mills, J. N., *Satellite imagery characterizes local animal reservoir populations of Sin Nombre virus in the southwestern United States*, Proc. Nat. Ac. Sci. **99**, 16817-16822 (2002).

[27] Glass, G. E., Shields, T. M., Parmenter, R. R., Goade, D., Mills, J. N., Cheek, J., Cook J. and Yates, T. L., *Predicted Hantavirus risk in 2006 for the southwestern U. S.*, Ocasional Papers, Museum of Texas Tech University **255**, 1-16 (2006).

[28] Ostfeld R. S. and Holt, R. D., *Are predators good for your health? Evaluating evidence for top-down regulation of zoonotic disease reservoirs*, Frontiers in Ecology and the Environment **2**, 13-20 (2004).

[29] Packer, C., Holt, R. D., Hudson, P. J., Lafferty, K. D. and Dobson, A. P., *Keeping the herds healthy and alert: implications of predator control for infectious disease*, Ecol. Lett. **6**, 797-802 (2003).

[30] Risken, H., *The Fokker-Planck Equation: Methods of solution and applications*, Springer-Verlag, New York (1989).

[31] van Kampen, N. G., *Stochastic Processes in Physics and Chemistry*, Elsevier Sience B.V., Amsterdam, (2003).

[32] Nåsell, I., *Stochastic models of some endemic infections*, Math. Biosc. **179**, 119 (2002).

[33] Peters, C. J., Mills, J. N., Spiropoulou, C. F., Zaki, S. R. and Rollin, P. E., in *Tropical Infectious Diseases*, Guerrant, R. L. and Weller, P. F. (Eds.), chap. 113, p. 1217, W. B. Saunders, New York, USA (1999).

[34] Suzán, G., Marcé, E., Parmenter, R. R., Giermakowski, J. T., Mills, J., Armien, B., Armien, A., Pascale, J. M., Zaldivar, Y., Salazar, J. and T. L. Yates, *Responses of hantavirus host communities in Panama to species removal*. Presented at the 84th Annual Meeting of the American Society of Mammalogists. 12-16 June 2004. Humboldt State University, Arcata, California, USA.

[35] Suzán, G., *The responses of Hantavirus host communities to habitat fragmentation and biodiversity in Panama*, Ph. D. dissertation, University of New Mexico, Albuquerque, NM, USA, (2005).

[36] Botten, J., Mirowsky, K., Ye, C., Gottlieb, K., Saavedra, M., Ponce, L. and Hjelle, B., *Shedding and intracage transmission of Sin Nombre Hantavirus in the deer mouse (*Peromyscus maniculatus*) model*, J. Virology **76**, 75877594 (2002).

[37] Mills, J. N., Yates, T. L., Ksiazek, T. G., Peters, C. J. and Childs, J. E., *Long-term studies of Hantavirus reservoir populations in the Southwestern United States: Rationale, potential, and methods*, Emerging Infectious Diseases **5**, 95-101 (1999).

[38] Begon, M., Townsend C. R. and Harper, J. L., *Ecology: From Individuals to Ecosystems*, Blackwell (2006).

[39] Tilman, D., May, R., Lehman, C. L. and Nowak, M. A., *Habitat destruction and the extinction debt*, Nature **371**, 65-66 (1994).

[40] McKane, A. J. and Newman, T. J., *Predator-prey cycles from resonant amplification of demographic sstochasticity*, Phys. Rev. Lett. **94**, 218102 (2005).

[41] Gillespie, D. T., *A general method for numerically simulating the stochastic time evolution of coupled chemical reactions*, J. Comp. Phys. **22**, 403-434 (1976).

[42] Gillespie, D. T., *Exact stochastic simulation of coupled chemical reactions*, J. Phys. Chem. **81**, 2340-2361 (1977).

[43] Nåsell, I., *On the quasi-stationary distribution of stochastic logistic epidemic*, Math. Biosc. **156**, 21-40 (1999).

[44] Aparicio, J. P. and Solari, H. G., *Sustained oscillations in stochastic systems*, Math. Biosciences **169**, 15-25 (2001).

[45] Wilson, E. B. and Lombard, O. M., *Cycles in measles and chicken pox*, Pathology **31**, 367-371 (1945).

[46] Bartlett, M. S., *Measles periodicity and comunty size*, J. R. Stat. Soc. A **120**, 48-70 (1957).

[47] Risau-Gusmán, S. and Abramson, G., *Oscillations in two-species models: tying the stochastic and deterministic approaches*, Eur. Phys. J. B (in press, 2008).